ALKALI-ACTIVATED SLAG MORTARS CONTAINING ALTERNATIVE ACTIVATOR: LONG-TERM MECHANICAL FRACTURE PARAMETERS

Hana ŠIMONOVÁ[1], *Barbara KUCHARCZYKOVÁ*[1], *Vlastimil BÍLEK, Jr.*[1, 2], *Dalibor KOCÁB*[1]

[1] Brno University of Technology, Faculty of Civil Engineering, Veveří 331/95, 602 00 Brno, Czech Republic
[2]Brno University of Technology, Faculty of Chemistry, Purkyňova 464/118, 612 00 Brno, Czech Republic

simonova.h@vutbr.cz, barbara.kucharczykova@vutbr.cz, bilek@fch.vut.cz, dalibor.kocab@vutbr.cz

DOI: 10.35181/tces-2020-0014

Abstract. *This paper deals with the determination of long-term mechanical fracture properties of alkali-activated slag (AAS) mortars with the alternative activator. Waste sludge from the production of waterglass was used as a sole alkaline activator for ground granulated blast furnace slag. Two types of sand were used to prepare two different mortar sets: standardized siliceous CEN sand consisting of three fractions according to EN 196-1 and natural sand with a nominal grain size up to 4 mm. The results of the elastic, fracture and strength parameters for both sets of AAS mortars determined within the time interval of 3 to 650 days of ageing are summarized in the paper. The obtained results show a different trend in the development of the material properties of AAS mortars compared to the ordinary cement-based mortars which should be taken into the account in the material specification for practical application. It seems that the hardening process influencing the mechanical fracture characteristics is more progressive after the age of 28 days.*

Keywords

Alkali-activation, fracture, mortar, slag, waste sludge.

1. Introduction

The traditional way to increase the sustainability of a building industry includes particularly as largest as a possible replacement of Portland clinker content in different types of cement and concrete by suitable natural or industrial pozzolans and latent hydraulic materials. Nevertheless, these materials are usually suitable to be alkali-activated to obtain even clinker-free binders offering high mechanical properties, relatively low hydration heat, resistance to aggressive environments, and elevated temperatures [1].

However, the sustainability of alkali-activated materials (AAMs) can be questioned due to energetically and ecologically demanding production of alkaline activators that are usually sodium or potassium waterglasses and hydroxides. Therefore, the use of various alkaline industrial wastes instead of the pure activators is in research interest. These include cleaning solution from aluminium foundry industry [2] or partial dissolution of waste glass in NaOH solution before alkaline activation of suitable precursor [3] to enrich the activating solution with dissolved silicates and thus make more efficient waterglass-like activator.

In the present study, waste sludge from the waterglass production was used as an alternative alkaline activator. After the dissolution of siliceous sand in sodium hydroxide solution at elevated temperature and pressure, filtration process follows. Unlike most of pure concentrated waterglass, the sludge consisting of unreacted sand and the rest of waterglass does not pass the filter and is further discarded as waste. Therefore, the composition of the liquid phase in the sludge is the same as the produced raw waterglass, but diluted with solid content and hence, the sludge can even fully replace alkaline activator but part of fine aggregates as well. Both benefits make this alternative activator very interesting for the use in AAMs. On the other hand, handling with sludge can be complicated by fluctuations in the solid content from batch to batch results in its variable consistency from very stiff concentrated suspension prone to sedimentation to homogenous “wet powder-like”. This study is more specifically focused on the determination of long-term mechanical fracture properties of alkali-activated slag mortars with the described alternative activator.

2. Experiment

2.1. Materials

Waste sludge from the production of waterglass was used as a sole alkaline activator for ground granulated blast furnace slag. Sludge consisted of 72.1% solids (siliceous sand), 4.1% Na_2O, 7.3% SiO_2 and 16.5% water. Sludge to slag ratio was 1.95:1 to adjust the Na_2O dose to 8% by slag weight. Blast furnace slag consisted predominantly of amorphous phase (about 90%) while the rest was calcite, akermanite and merwinite. Blaine fineness of slag was 400 m^2/kg. Two types of sand were used to prepare two different mortar sets: standardized siliceous CEN sand consisting of three fractions according to EN 196-1 [4] (corresponding mortar set denoted as "*S*") and natural sand (locality Žabčice) with a nominal grain size up to 4 mm (corresponding mortar set denoted as "*N*"). Fine aggregate to slag ratio was 3:1, where fine aggregate consists of the given type of sand and the solid content from waste sludge. The high amount of waste sludge introduced into the mortars resulted in increased water demand of these mortars and hence the water to slag ratio was 0.73 and 0.98 for *S* and *N* mortar, respectively.

2.2. Specimens and curing conditions

The Hobart mixer was used for the mixing of particular components. The mixing process took approximately 8 minutes. At first, the waste sludge and water were mixed to prepare a homogeneous activating solution. Afterwards, the slag and finally the sand was added. The basic properties of fresh mortars are introduced in Tab.1 The consistency of fresh mortars was determined based on a flow table test using a conical mould with a diameter of the top and bottom opening of 70 and 100 mm, and with a height of 60 mm, according to ČSN EN 1015-3 [5]. The bulk density of fresh mortars was determined according to ČSN EN 1015-6 [6]. The air content of fresh mortars was determined using the device according to ČSN EN 1015-7 [7]. The air content was measured at the start and at the end of pouring mortars into the moulds. Both mortars exhibited a decrease of the air content, an average value is introduced in Tab.1

The mortars were cast into the ultra-high-molecular-weight polyethylene moulds (Hakorit) for preparation of prismatic specimens with nominal dimensions of 40 × 40 × 160 mm. The moulds were sealed with a PE foil for 24 hours at a temperature of 21 ± 2 °C. Afterwards, the specimens were demoulded and stored in an air-conditioned room where the temperature of 21 ± 2 °C and relative humidity of 50 ± 10% were maintained.

Tab. 1: Basic characteristics of fresh mortars.

Mixture	Spread (mm) after		Bulk	Air content
	lifting the cone	15 jolts		
S	160	235	2130	3.2
N	120	170	2070	4.2

2.3. Measurement of length changes

The shrinkage process of both mortars was determined based on the measurement of length changes. The prismatic specimens of above-mentioned dimensions with special markers embedded into the ends of the test specimens (in the longitudinal axis of the specimens) were used for this purpose. The measurement was started immediately after the demoulding of the specimens at the age of 24 hours. The length changes of both sets of specimens were measured in regular intervals using the measurement gauge equipped with the digital probe with a resolution of 0.001 mm. Simultaneously, the mass losses due to the specimens' desiccation were recorded. Details about the development of shrinkage values in time can be found in [8]. Especially, detailed results of short-term shrinkage behaviour were introduced and discussed. In this paper, only the selected results of length change measurement related to the results of fracture tests are presented.

2.4. Resonance method

During the specimens ageing, the dynamic modulus of elasticity was monitored and determined using the resonance method according to the standard ČSN 73 1372 [9]. The natural frequency of longitudinal vibration was determined for each specimen. The vibration was generated by a mechanical impulse using the impact hammer and the natural frequency was measured by an oscilloscope Handyscope HS4 with a piezoelectric sensor. The dynamic modulus of elasticity E_{dyn} was then calculated from this natural frequency according to the standard [9].

2.5. Fracture tests

The fracture tests of prismatic specimens with an initial notch were performed at the age of 3, 28, 107, 330 and 650 days. The three specimens were tested at each investigated age for each mortar set. The specimens were tested under the three-point bending configuration (see Fig. 1). The span length was set to 120 mm. The depth of the initial notch was, in this case, approx. 1/3 of the specimen's height. The specimens were subjected to the quasi-static loading using a very stiff multi-purpose mechanical testing machine LabTest 6.250 with the load range of 0−250 kN with a constant displacement increment of 0.02 mm/min.

During the fracture tests, the vertical displacement *d* (mid-span deflection) was measured using the inductive sensor mounted in a special measuring frame placed on the specimens (see Fig. 1). Crack mouth opening displacement (*CMOD*) was measured using a displacement transducer mounted between blades fixed on the bottom surface of the test specimens, close to the initial notch (see Fig. 1). Simultaneously, the vertical force *F* was recorded. In this way continual record of *F–d* and *F−CMOD* diagrams of the loading tests were obtained. The raw data were subsequently processed for the purpose of the evaluation of the fracture characteristics. At first, the adjustment of

raw measured *F–d* and *F−CMOD* diagrams was performed to obtain the appropriate input values for their subsequent evaluation. The GTDiPS software [10] was used for this purpose. This procedure includes several steps. Particularly the shifting of the origin of the coordinate system, the smoothing of the diagram and the reduction of the number of points. A chain of transformation steps has been put together in the software for this purpose. The *F–d* and *F−CMOD* diagrams after the advanced correction for both sets of specimens at investigated ages are shown in Fig. 2 and Fig. 3, respectively. Note that in the case of *F−CMOD* diagrams only the part until a peak load is used for subsequent evaluation, therefore only the part of the whole range of measurement is displayed in Fig. 3.

Fig. 1: Arrangement of the fracture test.

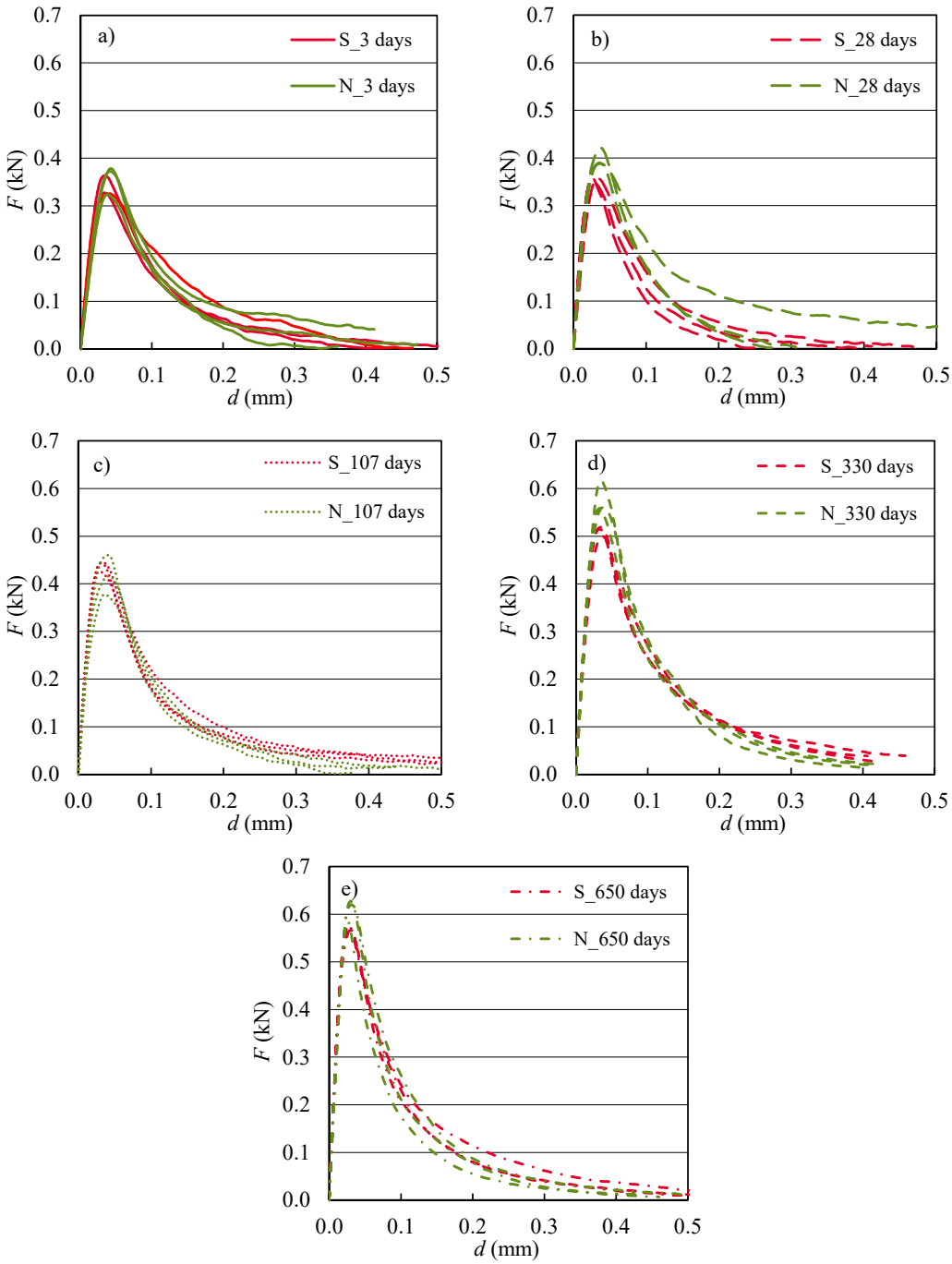

Fig. 2: The *F–d* diagrams for both sets of specimens at investigated ages: a) 3 days, b) 28 days, c) 107 days, d) 330 days, and e) 650 days.

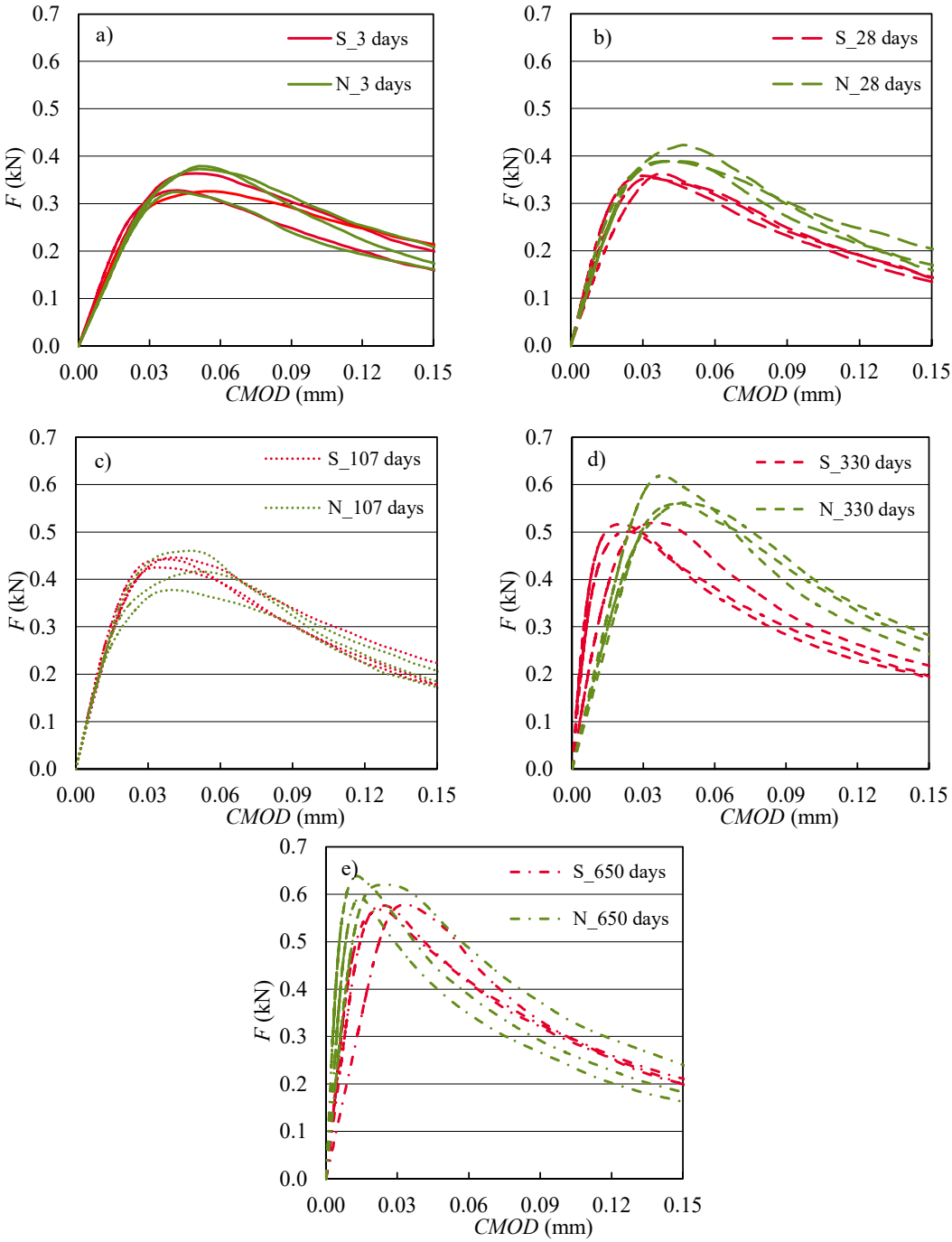

Fig. 3: The *F–CMOD* diagrams for both sets of specimens at investigated ages: a) 3 days, b) 28 days, c) 107 days, d) 330 days, and e) 650 days.

Subsequently, the mechanical fracture parameters were determined based on the direct evaluation of fracture test records using the selected fracture models. The modulus of elasticity values were estimated from the initial parts of *F–d* diagrams according to [11]. The effective crack length, corresponding to the maximum load and matching mid-span deflection, was calculated to determine the fracture toughness value. The fracture toughness value was determined using the effective crack model according to [11] which combines the linear elastic fracture mechanics and crack length approaches. The work of fracture value was calculated from the whole *F–d* diagrams according to the RILEM method [12] and corresponds to the area under the *F–d* diagram. Afterwards, the specific fracture energy value was determined, that the work of fracture value was divided by the ligament area (cross-section of specimens through which the crack grows).

The *F–CMOD* diagrams were evaluated using the double-*K* fracture model. The advantage of this model is that it can predict the crack initiation, stable crack propagation, and unstable fracture process that occurs during the crack propagation in a quasi-brittle material. According to this criterion, two parameters, initial cracking toughness and unstable fracture toughness can be used to predict different stages of the fracture process. This

model is based on a combination of the concept of cohesive forces acting on the faces of the fictitious (effective) crack increment with a criterion based on the stress intensity factor (details can be found in [13]). The unstable fracture toughness is defined as the critical stress intensity factor, which is similar to effective fracture toughness used in the effective crack model by Karihaloo [11]. Apart from unstable fracture toughness, the cohesive fracture toughness has to be calculated to determine initial cracking toughness. The cohesive softening function describing the relationship between cohesive stress and effective crack opening displacement needs to be determined. Based on the own preliminary study it can be stated that the type of softening function (bilinear or nonlinear) has no significant effect on the calculated values of fracture parameters [14]. Therefore, the nonlinear softening function according to Reinhardt [15] was considered in this paper. The input parameters of softening function are more important, especially the way of estimation of tensile strength. Commonly, the compressive strength value is used for estimation of the tensile strength of the material. More appropriate is to determine the tensile strength directly from the tensile test performed in the configuration most similar to the loading of the real structural element, i.e. flexural strength in the case of three-point bending test. Another way is the estimation of the tensile strength via inverse analysis based on the artificial neural network. It is expected that in this case the value corresponds to the uniaxial tensile strength of the material which is usually used as the input value for the design of the structures. Therefore, for the purpose of double-*K* fracture model the values of identified tensile strength was considered. The details about the procedure of parameters identification can be found in [16].

Note that the informative compressive strength value was determined on the fragments remaining after the fracture experiments had been performed. The informative flexural strength value was calculated from the maximum force obtained during the fracture test.

3. Results

The development of dynamic modulus of elasticity and shrinkage process was monitored during the specimens ageing. These parameters were measured at regular intervals until their steady-state. Table 2 introduces the values of these parameters for both sets of AAS mortars in selected age of specimens near to the age when fracture tests were performed. The significant increase of dynamic modulus of elasticity was achieved within the time interval 2 and 27 days for both mortar sets. The increase of this parameter after 27 days up to steady-state value was less than 15% for both sets of AAS mortars. The trend of shrinkage development during the specimen's ageing is similar to the development of dynamic modulus of elasticity. The most of the shrinkage occurred during the first 28 days after which the values for both mortars was already stabilized. More details about the development of shrinkage values during the whole interval of measurement can be found in [8]. Because both parameters are strongly affected by the actual level of internal humidity of tested specimens, the trend of their development can be estimated very well from the development of the mass losses recorded during specimens ageing. The results show very good correspondence between the trend of development of dynamic modulus of elasticity and shrinkage with the trend of recorded mass losses which were almost stabilized for both mortars at the age of 27 days (see Table 2). It is worth noting that, at later stages (after 178 and 350 days, respectively), mass losses are stopped, while slight shrinkage carries on. This correlates well with a simultaneous increase in the bulk density (Table 3). This phenomenon can be related to the carbonation, but also to creep as well as shrinkage originating from ongoing hydration reactions that are manifested by increased basic mechanical properties as well as most of mechanical fracture properties.

Besides the bulk density, Table 3 presents some other values of the basic characteristics of hardened AAS mortars. The average values (determined based on 3 independent measurements) and coefficient of variations (CoV in %) are presented. The informative compressive and flexural strength values gradually increased with the specimen's age for both sets of AAS mortars. The compressive strength increased about 13 and 26% within the time interval 28 to 330 days for mortar set *S* and *N*, respectively. The mortar set *N* exhibited slightly lower values of compressive strength with higher variability compared to the set *S* during the whole monitored time interval. The differences decreased with the specimens ageing. On the contrary, the flexural strength value was about 10% higher for mortar set *N* in comparison with set *S* during the whole monitored time interval. The exception was observed at the age of 107 days when the values are the same if the variability is taken into the account. The flexural strength increased about 50% within the time interval 28 to 650 days for both sets of AAS mortars. Concerning the tensile strength determined via inverse analysis and flexural strength calculated by direct evaluation, a similar trend of development is obtained for both characteristics of particular AAS mortars. When the absolute values are compared for the particular ages of specimens, the flexural strength is in most cases about 55 % higher compared to tensile strength.

Tab. 2: Mean values (CoV in %) of dynamic modulus of elasticity, length changes and mass losses – set *S* and *N*.

		Age of specimens (days)				
Parameter	**Unit**	**2**	**27**	**93**	**178**	**650**
Dynamic modulus of elasticity	GPa	6.0 (2.5)	9.8 (2.4)	10.7 (2.0)	11.0 (2.1)	–
		3.0 (3.1)	9.4 (4.6)	10.1 (4.1)	10.7 (2.7)	–
Shrinkage	mm/m	10.0 (6.6)	16.3 (1.2)	16.6 (1.2)	16.7 (1.2)	16.8 (1.2)
		6.9 (4.7)	15.7 (1.6)	16.0 (1.6)	16.1 (1.6)	16.2 (1.6)
Mass losses	%	5.1 (0.4)	8.5 (0.7)	8.8 (0.7)	8.9 (0.7)	8.9 (0.7)
		5.9 (0.6)	10.1 (0.5)	10.5 (0.3)	10.6 (0.3)	10.6 (0.3)

Tab. 3: Mean values (CoV in %) of basic characteristics of hardened mortars – set *S* and *N*.

Parameter	Unit	Age of specimens (days) 3	28	107	330	650
Bulk density	kg/m^3	2060 (0.3)	1990 (0.8)	2000 (0.3)	2000 (0.6)	2020 (0.5)
		1970 (0.7)	1900 (0.5)	1890 (0.3)	1900 (0.6)	1940 (0.5)
Compressive strength	MPa	15.9 (3.1)	17.9 (1.8)	19.4 (3.4)	20.3 (2.0)	–
		12.4 (2.6)	14.9 (3.5)	16.7 (9.2)	18.8 (3.7)	–
Flexural strength	MPa	2.10 (6.7)	2.29 (3.1)	2.76 (2.3)	3.19 (1.9)	3.51 (0.2)
		2.27 (9.7)	2.54 (4.3)	2.65 (10.9)	3.58 (4.7)	3.8 (3.5)
Identified tensile strength	MPa	1.34 (16.3)	1.48 (7.5)	1.67 (5.6)	2.04 (3.4)	2.28 (3.5)
		1.71 (13.5)	1.64 (14.5)	1.69 (19.9)	2.59 (11.5)	2.78 (3.3)

Figs. 4−8 show the average values (determined based on 3 independent measurements) and sample standard deviations (given by the error bars) of the monitored mechanical fracture parameters of AAS mortars determined from *F–d* and *F–CMOD* diagrams using the non-linear fracture models described in section 2.5. The mechanical fracture parameters were determined at the specimens age of 3, 28, 107, 330, and 650 days.

Based on the evaluation of fracture tests it can be observed that the modulus of elasticity increased by 60% for both sets of AAS mortars within the age interval from 28 to 650 days (see Fig. 4). The highest values achieved were about 14 GPa and 13 GPa at the age of 650 days for mortar set *S* and *N*, respectively. The effective fracture toughness values also gradually increased with the specimen's age for both sets of AAS mortars. The fracture toughness increased by 63 and 30% for mortar set *S* and *N*, respectively, within the age interval from 28 to 650 days (see Fig. 5). The highest values achieved were about 0.5 MPa·m$^{1/2}$ for both sets of AAS mortars at the age of 650 days. The specific fracture energy value gradually increased between the age of 3 and 330 days for mortar set *N*. The highest value 66 J/m^2 was achieved at the age of 330 days and it is about 58% higher in comparison with value at the age of 3 days. At the age of 650 days, the decrease by 17% was observed but the variability is 2 times higher in comparison with the age of 330 days. In the case of mortar set *S*, the fracture energy value decreased between the age of 3 and 28 days. After that, the gradual increase with specimen's age was monitored. The increase was about 70% when the values are compared at the age of 28 and 650 days (see Fig. 6).

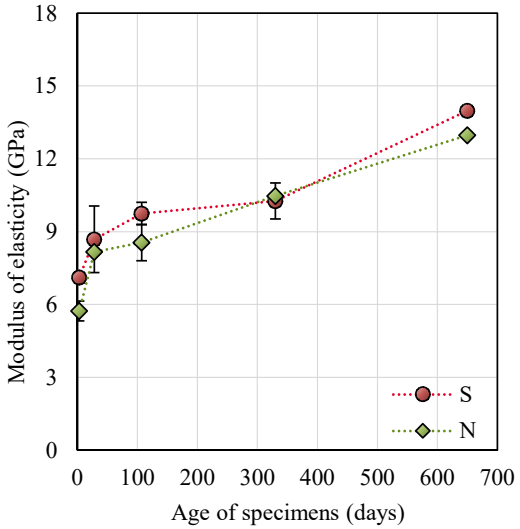

Fig. 4: The modulus of elasticity values for both sets of AAS mortars.

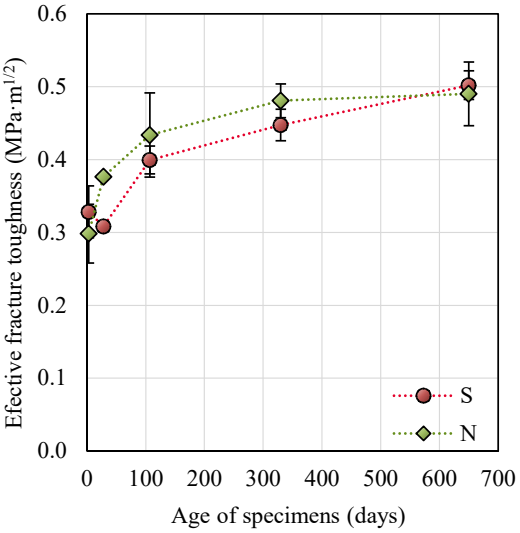

Fig. 5: The effective fracture toughness values for both AAS mortars.

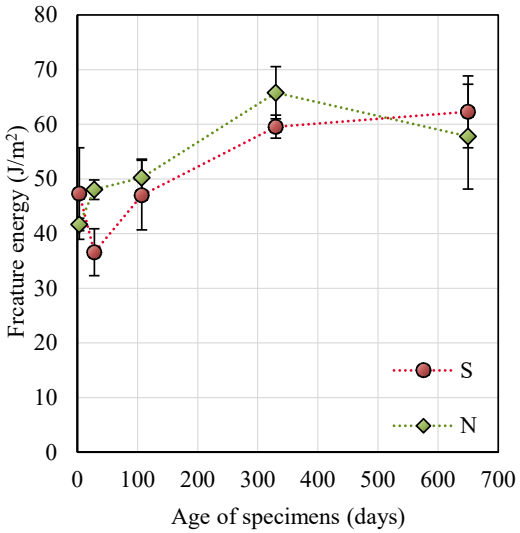

Fig. 6: The specific fracture energy values for both sets of AAS mortars.

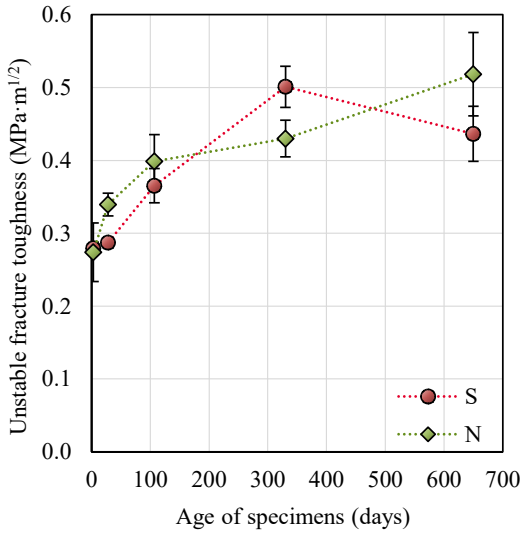

Fig. 7: The unstable fracture toughness values for both sets of AAS mortars.

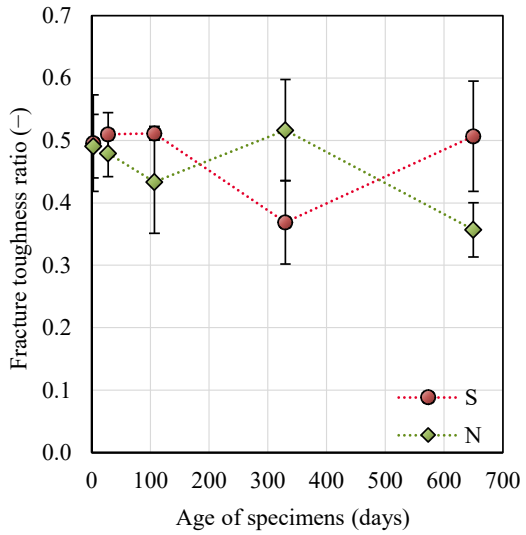

Fig. 8: The fracture toughness ratio for both sets of AAS mortars.

Both sets of AAS mortars exhibited the same trend of the development of the values of unstable fracture toughness within the time interval from 28 to 107 days as in the case of effective fracture toughness value. The different trend was observed within the time interval from 107 to 650 days for both sets of AAS mortars. When we compare the absolute values of fracture toughness determined by two different fracture models for the particular ages of specimens, the difference is in most cases about 10% (see Figs. 5 and 7). Fig. 8 shows the resistance of the material to the stable crack propagation, which is here expressed by the ratio of initial cracking toughness and unstable fracture toughness. No trend is observed in the development of this parameter during the specimens' ageing for both sets of AAS mortars. This parameter exhibits the highest variability of results.

4. Conclusion

The results of fracture tests evaluation of two sets of AAS mortars made from slag activated by the waste sludge from waterglass production were presented in this paper. The main attention was focused on monitoring the mechanical fracture parameters values during the specimens ageing within the time interval of 3 to 650 days.

The dynamic modulus of elasticity and shrinkage values exhibited significant increase within the time interval of 2 and 27 days with the absolute values, determined at the age of 27 days, more than 85% of total long-term values. On the contrary, the values of monitored mechanical fracture parameters significantly increased within the time interval of 28 to 650 days. The obtained results show a different trend in the development of the material properties of AAS mortars compared to the ordinary cement-based mortars which should be taken into the account in the material specification for practical application. It seems that the hardening process influencing the mechanical fracture characteristics is more progressive after the age of 28 days. Simultaneously, the early stage of hardening is under the risk of massive shrinkage.

Acknowledgements

This outcome has been achieved with the financial support of the Czech Science Foundation under project No 18-12289Y. The authors would like to express their special thanks to Martin Lipowczan from Brno University of Technology for conducting the identification of mechanical fracture parameters of which results were partially used as input data for direct evaluation in this paper.

References

[1] PROVIS, J. L. and J. S. J. VAN DENVENETR, eds, *Alkali activated materials: state-of-the-art report, RILEM TC 224-AAM*. Dordrecht: Springer, 2014. ISBN 978-94-007-7672-2.

[2] FERNÁNDEZ-JIMÉNEZ, A., N. CRISTELO, T. MIRANDA and Á. PALOMO. Sustainable alkali activated materials: Precursor and activator derived from industrial wastes. *Journal of Cleaner Production*. 2017, vol. 162, pp. 1200–1209. ISSN 0959-6526. DOI: 10.1016/j.jclepro.2017.06.151

[3] TORRES-CARRASCO, M. and F. PUERTAS. Waste glass in the geopolymer preparation. Mechanical and microstructural characterisation. *Journal of Cleaner Production*. 2015, vol. 90, pp. 397–408. ISSN 0959-6526. DOI: 10.1016/j.jclepro.2014.11.074

[4] ČSN EN 196-1. *Methods of testing cement – Part 1: Determination of strength.* Prague: ÚNMZ, 2016.

[5] ČSN EN 1015-3. *Methods of test for mortars for masonry – Part 3: Determination of consistence of fresh mortar (by flow table).* Prague: ÚNMZ, 2000.

[6] ČSN EN 1015-6. *Methods of test for mortars for masonry – Part 6: Determination of bulk density of fresh mortar.* Prague: ÚNMZ, 1999.

[7] ČSN EN 1015-7. *Methods of test for mortars for masonry – Part 7: Determination of air content of fresh mortar.* Prague: ÚNMZ, 1999.

[8] KUCHARCZYKOVÁ, B., V. BÍLEK, Jr. and H. Šimonová. Shrinkage of the alkali-activated slag mortars containing alternative activator. *IOP Conf. Series: Materials Science and Engineering*. 2019, vol. 660, 012001. ISSN 1757-899X, 1757-8981. DOI:10.1088/1757-899X/660/1/012001

[9] ČSN 73 1372. Non-destructive testing of concrete – Testing of concrete by resonance method. Prague: ÚNMZ, 2012.

[10] FRANTÍK, P. and J. MAŠEK. *GTDiPS software*, 2015. Available at: http://gtdips.kitnarf.cz/

[11] KARIHALOO, B. L. *Fracture Mechanics and Structural Concrete*. New York: Longman Scientific & Technical 1995. ISBN 978-0582215825

[12] RILEM TC – 50 FMC (Recommendation): Determination of the fracture energy of mortar and concrete by means of three-point bend test on notched beams. *Materials and Structures*. 1985, vol. 18, iss. 4, pp. 287–290. ISSN 1359-5997. DOI: 10.1007/BF02472918

[13] KUMAR, S. and S. C. BARAI. *Concrete Fracture Models and Applications*. Berlin: Springer, 2011. DOI: 10.1007/978-3-642-16764-5

[14] ŠIMONOVÁ, H., KUCHARCZYKOVÁ, B., KERŠNER, Z., MERTA, I., POLETANOVIĆ, B., MALÍKOVÁ, L., SEITL., S. Effect of softening function type in double-*K* fracture model: Alkali-activated fly ash mortar with hemp fibres. In: PIJAUDIER-CABOT, G., P. GRASLL and C. LA BORDERIE, eds. *FraMCoS-X 10th International Conference on Fracture Mechanics of Concrete and Concrete Structures*. France: IA-FraMCoS, 2019, pp. 1−98. DOI: 10.21012/FC10.232513

[15] REINHARDT, H. W., H. A. W. CORNELISSEN and D. A. HORDIJK. Tensile tests and failure analysis of concrete. *Journal of Structural Engineering*. 1986, Vol. 112, pp. 2462–2477. ISSN 0733-9445. DOI: 10.1061/(ASCE)0733-9445(1986)112:11(2462)

[16] LEHKÝ, D., M. LIPOWCZAN, H. ŠIMONOVÁ and Z. KERŠNER. A neural network ensemble for the identification of mechanical fracture parameters of fine-grained brittle matrix composites. In: PIJAUDIER-CABOT, G., P. GRASLL and C. LA BORDERIE, eds. *FraMCoS-X 10th International Conference on Fracture Mechanics of Concrete and Concrete Structures*. France: IA-FraMCoS, 2019, pp. 1−9. DOI: 10.21012/FC10.234717

About Authors

Hana ŠIMONOVÁ was born in Slaný, Czech Republic. She received her B.Sc., M.Sc. and PhD. degrees in Civil Engineering from Brno University of Technology, Faculty of Civil Engineering (BUT), Czech Republic in 2008, 2010, and 2013, respectively. Her current research interests include fatigue and fracture mechanics of quasi-brittle composites field, evaluation of fatigue and static fracture tests of many different types of materials based on brittle matrix.

Barbara KUCHARCZYKOVÁ was born in Třinec, Czech Republic. She received the M.Sc., PhD. and Assoc. Prof. degrees in Civil Engineering from the Brno University of Technology (BUT) in 2003, 2008, and 2020, respectively. Her current research interests include the technology of production of cement composites, design and implementation of experimental analysis and testing methods used for measurement and evaluation of the characteristics of building materials.

Vlastimil BÍLEK, jr. was born in Vyškov, Czech Republic. He received his B.Sc, M.Sc. and PhD. degrees from BUT (Faculty of Chemistry) in 2011, 2013, and 2017, respectively. His research interests include research and development of non-traditional binders, particularly alkali-activated materials, monitoring their hydration and the application of both organic and inorganic additives to these systems.

Dalibor KOCÁB was born in Brno, Czech Republic. He received the M.Sc. and PhD. degrees in Civil Engineering from the Brno University of Technology (BUT) in 2008, and 2016, respectively. His main area of research focuses on non-destructive testing, particularly on the ultrasonic pulse velocity test and resonance method.